

UC San Diego

Independent Study Projects

Title

Patient-specific 3D models aid planning for triplane proximal femoral osteotomy in slipped capital femoral epiphysis

Permalink

<https://escholarship.org/uc/item/6p43g5vj>

Authors

Cherkasskiy, Lillia
Caffrey, J. P.
Szewczyk, A. F.
et al.

Publication Date

2018

Peer reviewed

Patient-specific 3D models aid planning for triplane proximal femoral osteotomy in slipped capital femoral epiphysis

L. Cherkasskiy¹
J. P. Caffrey¹
A. F. Szewczyk¹
E. Cory¹
J. D. Bomar²
C. L. Farnsworth²
M. Jeffords²
D. R. Wenger²
R. L. Sah¹
V. V. Upasani²

Abstract

Purpose Slipped capital femoral epiphysis (SCFE) can result in a complex three-dimensional (3D) deformity of the proximal femur. A three-plane proximal femoral osteotomy (TPFO) has been described to improve hip mechanics. The purpose of this study was to evaluate the benefits of using 3D print technology to aid in surgical planning.

Patients and Methods Fifteen children treated with TPFO for symptomatic proximal femoral deformity due to SCFE were included in this study. Ten patients were treated by a single surgeon with (model group, n = 5) or without (no-model group, n = 5) a 3D model for pre-operative planning, and compared with patients treated by two senior partners without the use of a model (senior group, n = 5) to evaluate for a learning curve. Peri-operative data including patient body mass index (BMI), surgical time and fluoroscopy time were recorded.

Results Children in all three groups had similar BMIs at the time of the TPFO. Post-operative radiographic parameters were equally improved in all three groups. On average, surgical time decreased by 45 minutes and 38 minutes, and fluoroscopy time decreased by 50% and 25%, in the model

group compared with the no-model and senior groups, respectively.

Conclusions Patient-specific 3D models aid in surgical planning for complex 3D orthopaedic deformities by enabling practice of osteotomies. Results suggest that 3D models may decrease surgical time and fluoroscopy time while allowing for similar deformity correction. These models may be especially useful to overcome steep learning curves for complex procedures or in trainee education through mock surgical procedures.

Cite this article: Cherkasskiy L, Caffrey JP, Szewczyk AF, Cory E, Bomar JD, Farnsworth CL, Jeffords M, Wenger DR, Sah RL, Upasani VV. Patient-specific 3D models aid planning for triplane proximal femoral osteotomy in slipped capital femoral epiphysis. *J Child Orthop* 2017;11:147-153. DOI 10.1302/1863-2548.11.170277

Keywords: slipped capital femoral epiphysis; triplane proximal femoral osteotomy; 3D printing; mock surgery; surgical planning

Background

Slipped capital femoral epiphysis (SCFE) is the most common hip disorder in adolescents aged nine to 16 years, with an annual incidence of 10.8 cases per 100 000 children.^{1,2} In cases of moderate to severe SCFE, a triplane proximal femoral osteotomy (TPFO) may be performed to improve hip mechanics. A TPFO has been described to correct the extension, varus and external rotation deformities characteristic of SCFE with low rates of femoral head avascular necrosis (AVN).³⁻⁹ A variety of other osteotomies have also been described to correct the deformity. Imhauser recommended a simple flexion osteotomy⁹ while Dunn recommended a basicervical closing wedge femoral neck osteotomy.³ Some authors have recommended internal rotation of the distal fragment, while others feel that this manoeuvre creates extra-articular greater trochanteric impingement against the pelvis.^{3,9-11} Regardless of the type of osteotomy used, deformity correction in SCFE can be complex due to the three-dimensional (3D) deformity present and the inability to visualise the epiphyseal-metaphyseal junction when a standard lateral approach to the femur is used.¹²

¹ Department of Bioengineering, University of California-San Diego, 9500 Gilman Drive MC 0412, La Jolla, CA 92093-0412, USA

² Rady Children's Hospital, 3020 Children's Way, MC 5062, San Diego, CA 92123, USA

Correspondence should be sent to: Vidyadhar Upasani, Rady Children's Hospital, 3020 Children's Way, MC 5062, San Diego, CA 92123, USA.
E-mail: vupasani@rchsd.org

In recent years, advances and rapid growth in additive manufacturing methods and devices have allowed for clinical applications, including preparation and training for orthopaedic procedures. A number of studies have reported using patient-specific 3D printed models for surgical planning, showing improved outcomes for patients with orthopaedic deformities.¹⁸⁻²² The use of a 3D model in preparation for corrective surgeries for congenital scoliosis decreased operation time in four out of five surgeries to correct congenital scoliosis.¹³ In a case study, a 3D model of a pelvis with a large chondrosarcoma allowed for the creation of custom osteotomy guides which aided tumour resection with adequate margins.¹⁴ A randomised laboratory trial comparing traditional preparation with 3D model preparation for distal radius osteotomy found that model use resulted in shorter operations with more precise correction of ulnar variance and radial inclination.¹⁵

Currently, there are no studies known to the authors using 3D printed models for surgical planning of a TPFO. On the basis of these recent orthopaedic studies, we hypothesised that TPFO planned with the aid of patient-specific, plastic 3D printed models for mock-surgery practice would decrease surgery and fluoroscopy time without sacrificing radiographically assessed accuracy of the correction.

Patients and methods

Patient selection and image acquisition

Institutional Review Board approval was obtained prior to initiating this study. All patients were enrolled from a single institution. To be included in this study, all patients required a diagnosis of a moderate or severe SCFE (defined by an epiphyseal-shaft angle (ESA) of more than 30°), a pre-operative CT scan of the pelvis and treatment by TPFO. Fifteen patients (seven male and eight female) with a median age of 13.5 years (11.0 to 17.6) were included in the study.

The indications for a TPFO were hip pain and impingement due to either a healed or stable SCFE according to the Loder classification, with moderate to severe deformity at the proximal head neck junction as defined by an ESA of more than 30° and physical examination findings of at least 30° of obligate external rotation and hip flexion limited to 70° or less. All patients underwent a pre-operative pelvic CT scan (GE HiSpeed VCT, 64 slice; Piscataway, NJ USA) with a near-isotropic slice thickness of 0.625 mm, as is the standard procedure for all patients undergoing TPFO surgery.

Ten patients were prospectively enrolled in this study: five were enrolled prior to the acquisition of the 3D model printer and therefore did not have a printed model, the other five participants were enrolled after the acquisition of the 3D model printer and had 3D models made from their CT scans to assist planning for TPFO surgery. All ten

patients were treated by the same surgeon. To evaluate for a learning curve effect, five additional patients that were treated by two senior surgeons were retrospectively included. These patients were chosen by evaluating the surgical database of two senior surgeons that perform TPFOs and including the five most recent patients that met our inclusion criteria. Age at TPFO, body mass index (BMI), surgical time (mins), intra-operative fluoroscopy (mins), estimated blood loss (EBL)^{16,17} (mL) and follow-up (mths) were calculated and recorded. EBL was calculated by multiplying the difference between pre-operative and post-operative haemoglobin by estimated blood volume and dividing that product by the average of pre-operative and post-operative haemoglobin.

Image processing

For the five patients who had 3D models created, their CT Image files were processed by segmentation, smoothing and conversion to stereolithography (STL) 3D printable format. For each patient's CT scan, Digital Imaging and Communication in Medicine (DICOM) image stacks were processed using MIMICS v17.0 (Materialise, Leuven, Belgium). Segmentation of the right and left proximal femurs was performed semi-automatically using thresholding and region-growing tools to isolate the proximal femur. Each femoral region was automatically smoothed (0.7 factor, five iterations) and then exported as 3D-printable STL files. The STL files were manually inspected using MeshLab v1.3.3 (Visual Computing Lab, ISTI-CNR) for noise speckles, which were removed. STL files were then optimised for 3D printing using NetFabb Basic v5.2.1 (NetFabb GmbH, Lufburg, Germany) using the automated mesh repair function. The optimised mesh was then imported into MeshMixer v10.9.297 (Autodesk, San Rafael, CA, USA) to merge the femur STL with a standardised 3D model of a 35 × 75 × 75 mm rectangular prism stand to facilitate mounting of the femur in a vice for the mock surgery.

3D model printing

Each resulting STL file was printed with Acrylonitrile Butadiene Styrene (ABS) on a desktop fused deposition modelling 3D printer (TAZ 4, Lulzbot, Loveland, CO, USA). Models were printed with a 20% honeycomb fill pattern with automatically generated supports. A pilot study was performed to select the most appropriate fill pattern and percentage, based on semi-quantitative evaluation of cut resistance similarity to bone by the lead surgeon when cutting samples of varying fill parameters and percentages.

Mock surgery

Prior to the model group patient surgeries, a mock TPFO surgery was performed on the plastic 3D model by the lead surgeon, mimicking the tools and cut approaches

used during surgery. Models were mounted in a vice and cut using a System Seven Precision Saw (Stryker, Kalamazoo, MI, USA). Based on evaluating the CT image and using clinical judgment, a wedge of plastic 'bone' was removed from the intertrochanteric region to allow for flexion and valgus correction of the proximal femur. The 3D model allowed the surgeon to visualise the head-neck junction and optimise the proximal femoral physeal orientation to obtain the desired correction. If a preliminary cut or removal of 'bone' wedge was inadequate for the desired anatomical correction during the mock surgery, additional cuts were made to achieve acceptable correction. The 3D model allowed 3D visualisation of the anatomical consequence of each cut and wedge removal. A Kirschner-wire was used to preserve the orientation of the femoral bone segments (Fig. 1).

Radiographic evaluation

Data were collected from pre-operative and post-operative patient radiographs by two independent observers. The measurements made were the ESA on lateral radiographs, neck-shaft angle (NSA), articular surface to trochanter distance (ATD) and medial proximal femoral angle (MPFA). Together, these four measurements were used to quantify the slip deformity in the coronal and sagittal planes. The ESA measured on the frog-lateral radiograph is a direct measure of the posterior displacement of the epiphysis. Recently it has been suggested that any posterior displacement is 'pathologic' and may be indicative of an asymptomatic SCFE.¹⁸ The remaining three angles are measured in the coronal plane. The NSA is a measure of varus femoral neck deformity that can occur secondarily in SCFE patients due to the slipped epiphysis.¹⁹ Normal measurements in children are 120° to 130°, whereas in SCFE, the femur neck becomes more varus, decreasing NSA. The ATD is an indirect measure of inferior displacement of the epiphysis.²⁰ It assesses the distance between the tip of the greater trochanter and the articular surface (normal around 2 cm). Finally, the MPFA is another indirect measure of inferior displacement of the epiphysis.²¹ It measures the angle

between the tip of the trochanter and the centre of the femoral head, which should be 90° normally and becomes diminished when the epiphysis slips inferiorly.

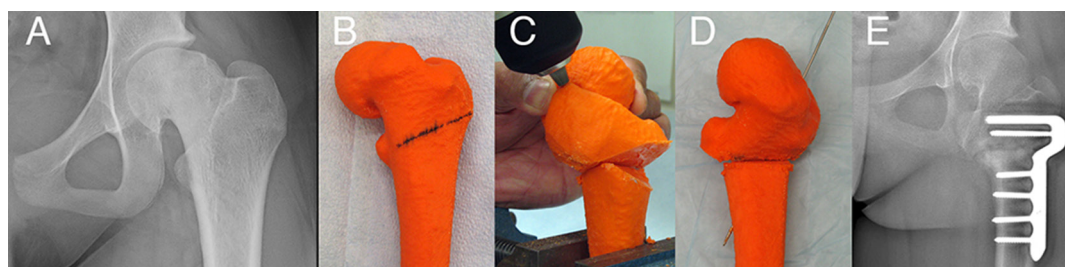
Statistical analysis

Pre-operative and post-operative data were analysed separately, and also as patient-specific differences. The intra-class correlation coefficient (ICC) was used to evaluate intra-observer agreement among the authors that measured the radiographs. Due to the small sample size in each group, data were evaluated using non-parametric techniques. The Kruskal-Wallis test was used to evaluate differences in the cohort. The Mann-Whitney test was used to evaluate differences among pairs in the cohort. The Wilcoxon signed ranks test was used to evaluate pre-operative to post-operative differences in radiographic measures. Statistical analysis was conducted using SPSS (v12, SPSS Inc., Chicago, IL, USA) with statistical significance threshold set to $p < 0.05$.

Results

Radiographic measurements were independently performed by two observers (the lead author and an orthopaedic surgery resident) and found to be similar (ICC scores range 0.81 to 0.98). Patients in all three groups were similar with respect to pre-operative characteristics (Table 1). The only pre-operative radiographic deformity that was statistically different among the three groups was ATD ($p = 0.04$), with the no model group being significantly lower than the senior group ($p = 0.02$). Follow-up varied among the three groups but was not found to be statistically significant ($p = 0.23$). The no-model group had a mean follow-up of 21 ± 10.8 months (10.3 to 32.1). The model group had a mean follow-up of 10.9 ± 4.8 months (4.3 to 17.9). The senior group had a mean follow-up of 37.1 ± 32.9 months (3.2 to 87.8).

Decrease in both surgical time and fluoroscopy time were observed in the model group, but were not found to be significant. Surgical time was decreased on average



©SD PedsOrtho

Fig. 1 (a) Pre-operative anteroposterior (AP) radiograph of a proximal femur of a 15-year-old girl with SCFE. (b) AP view of this patient's proximal femur 3D model, (c) the mock surgery osteotomies were performed and wedge removed and (d) fragments in final position. (e) A radiograph taken three months post-operatively indicates the correction achieved by the TPFO.

by 45 minutes in the model group compared with the no-model group, and 38 minutes compared with the senior group ($p = 0.40$). Fluoroscopy time decreased by 50% and 25% in the model group compared with the no-model and senior groups, respectively ($p = 0.30$, Table 2).

Patients in all three groups were similar with respect to post-operative characteristics (Table 3). The entire cohort saw statistically significant post-operative changes in ESA ($p = 0.001$, Table 4).

None of the patients in this study developed avascular necrosis; however, the follow-up period is limited. None of the patients in the model group developed post-operative complications or required additional surgery. One patient in the senior group was diagnosed with significant genu valgum and required a distal medial femoral hemiepiphyseodesis 11.2 months post TPFO procedure. Two patients in the no-model group had post-operative complications that required additional surgery. One patient had a mal-positioned implant and had a revision procedure one day after initial TPFO. The other patient underwent revision surgery 2.2 months following initial TPFO due to implant failure and went on to heal without further complication.

Discussion

Pre-operative planning is critically important when performing complex 3D corrections. Traditionally, surgical procedures have been planned using paper printed or traced radiographs and cut and paste methods to determine how the bone fragments would fit together. This is especially difficult in patients with SCFE as the relationship between the femoral epiphysis and metaphysis is displaced in all three dimensions (coronal, sagittal and axial), which cannot be appropriately represented on plain radiographs. Additionally, the magnitude of deformity in each plane varies between patients. The 3D print provides a unique opportunity to understand the deformity fully and to determine the patient-specific correction required to optimise hip mechanics. It is important to note that these improvements were achieved with relatively low 3D printing costs, which included a desktop 3D printer (one-time cost of ~\$2200) and plastic filament (~\$10 per patient model).

In the current study, we found that surgical time and fluoroscopy time for TPFO may be decreased by the use of patient-specific 3D models for mock surgery during

Table 1. Pre-operative parameters – Mean ± standard deviation (range).

	No-model group	Model group	Senior group	p-value
Age (yrs)	13.5 ± 2.5 (11.1 to 17.6)	14.1 ± 1.9 (11.8 to 16.1)	13.2 ± 1.6 (11 to 15.5)	0.79
BMI	29.6 ± 10.7 (18.7 to 42)	29.4 ± 6.2 (25 to 39.2)	27.0 ± 4.7 (18.9 to 30.6)	0.91
Pre-op ESA (°)	64 ± 20 (33 to 85)	65 ± 12 (53 to 81)	55 ± 15 (41 to 81)	0.33
Pre-op NSA (°)	136 ± 6 (129 to 145)	131 ± 13 (110 to 144)	136 ± 10 (125 to 151)	0.85
Pre-op ATD (mm)	5 ± 1 (4 to 7)	10 ± 11 (-7 to 21)	20 ± 12 (6 to 34)	0.04
Pre-op MPFA (°)	67 ± 7 (59 to 76)	73 ± 10 (57 to 82)	80 ± 10 (69 to 92)	0.22

ATD, articular surface to trochanteric distance; BMI, body mass index; ESA, epiphyseal slip angle; MPFA, medial proximal femoral angle; NSA, neck shaft angle

Table 2. Intra-operative parameters in minutes – Mean ± standard deviation (range).

	No-model group	Model group	Senior group	p-value
Surgical time (min)	170.4 ± 76.4 (107 to 257)	125.8 ± 25.4 (101 to 165)	163.8 ± 43.8 (125 to 238)	0.40
Fluoroscopy time (min)	0.6 ± 0.4 (0.2 to 1.2)	0.3 ± 0.3 (0.1 to 0.9)	0.4 ± 0.2 (0.2 to 0.6)	0.30
Estimated blood loss (mL)	962.6 ± 276.1 (626.8 to 1302)	979.8 ± 316.2 (694.5 to 1354.4)	981.5 ± 534.4 (174.3 to 1658.5)	0.95

Table 3. Post-operative parameters – Mean ± standard deviation (range).

	No-model group	Model group	Senior group	p-value
Post-op ESA (°)	20 ± 12 (7 to 37)	21 ± 9 (9 to 34)	18 ± 8 (8 to 29)	0.87
Post-op NSA (°)	130 ± 11 (118 to 140)	144 ± 13 (125 to 162)	133 ± 5 (128 to 140)	0.13
Post-op ATD (mm)	20 ± 11 (9 to 36)	20 ± 10 (6 to 30)	17 ± 8 (8 to 28)	0.78
Post-op MPFA (°)	78 ± 7 (70 to 89)	89 ± 10 (78 to 104)	74 ± 7 (65 to 80)	0.06

ATD, articular surface to trochanteric distance; ESA, epiphyseal slip angle; MPFA, medial proximal femoral angle; NSA, neck shaft angle.

Table 4. Pre-operative to post-operative changes for full cohort – Mean ± standard deviation (range).

	Pre-operative	Post-operative	p-value
ESA (°)	61 ± 16 (33 to 85)	19 ± 9 (7 to 37)	0.001
NSA (°)	135 ± 10 (110 to 151)	136 ± 12 (118 to 162)	0.46
ATD (mm)	12 ± 11 (-7 to 34)	19 ± 9 (6 to 36)	0.06
MPFA (°)	73 ± 11 (57 to 92)	80 ± 10 (65 to 104)	0.10

ATD, articular surface to trochanteric distance; ESA, epiphyseal slip angle; MPFA, medial proximal femoral angle; NSA, neck shaft angle

pre-operative planning. Although statistically insignificant, these reductions in surgical time and fluoroscopy time may be considered clinically significant. For example, an average decrease in operating room time of 45 minutes at our facility results in a saving of almost \$2700 per case. Given the drawbacks of pelvic fluoroscopy radiation, decreased trends with the model group shown in this study may greatly impact patient outcomes. The primary advantage of the model and mock surgery exercise was that the surgeon could gain a 3D understanding of each patient's specific proximal femoral deformity and determine the exact wedge of bone that would need to be removed from the intertrochanteric region to optimise the head-neck relationship and position of the proximal femoral physis. This allowed the surgeon to complete more efficiently the osteotomy (Fig. 2).

Similar post-operative radiographic outcomes in all three groups are an important finding. It may be that the sample size in each group was too small to detect a significant difference/improvement; however, it may also be due to the limitations of the TPFO osteotomy. The actual deformity created by a slipped femoral epiphysis occurs at the physis, however, the deformity correction of the TPFO is performed in the intertrochanteric region. While performing the osteotomy distal to the femoral neck is less risky to the tenuous blood supply from the epiphyseal retinacular vessels, there are limits to the amount of deformity correction that can be practically obtained.⁹ Also, this osteotomy creates a secondary 'Z'-shaped deformity at the femoral neck-shaft junction to improve the position of the femoral epiphysis. More recently, the modified Dunn procedure has been described that allows for SCFE deformity correction through the epiphysis.¹⁰ However, considering the femoral head avascular necrosis rate after this procedure is reported at 25% to 30% in stable slips,^{11,22} we believe the TPFO osteotomy is a more prudent treatment for this patient population.

Since follow-up time is markedly different between the three groups, as expected based on the study design, the

longer-term effect of model use remains to be established. There were 21 months of follow-up for the no-model group, 11 months for the model group and 37 months for the senior group. Comparing post-operative complications among the three groups, there was no AVN in any group, and no complications in the model group or the senior surgeon group. Two patients in the no-model group had complications that required surgical revision (one mal-positioned implant and one implant failure). These preliminary results suggest that 3D model use may decrease post-operative complications of TPFO, although further studies are needed to determine if this effect is statistically significant. These results may also be explained in part by a learning-curve effect, wherein the lead surgeon improved the surgical complication rate from 2/5 (no model) to match that of the senior surgeons when using 3D models (0/5). Therefore, the use of a 3D model mock surgery may be especially useful for training purposes.

The study had a number of limitations. The power of our statistical analysis was decreased because a small patient sample size was used (three groups of five patients each). This was primarily due to the low incidence of moderate to severe stable SCFE at a single institution and likely influenced our ability to detect significant differences in surgical time (effect size = 0.13, power = 0.07) and fluoroscopy time (effect size = 0.17, power = 0.08). In the current study, a single 3D model was used for each patient. Future studies may explore using multiple printed models to allow multiple mock surgeries to allow comparison of surgical corrections during planning. This study also did not examine reasons for shorter surgical times in the model group. We speculate that less time was spent in the operating room preparing for surgical cuts, as well as revising inadequate cuts.

As shown recently in other orthopaedic applications, 3D printed models can be an invaluable surgical tool to treat complex 3D orthopaedic deformities and improve surgical outcomes of TPFO. Tangible full-sized 3D models of the proximal femur allow for better understanding and

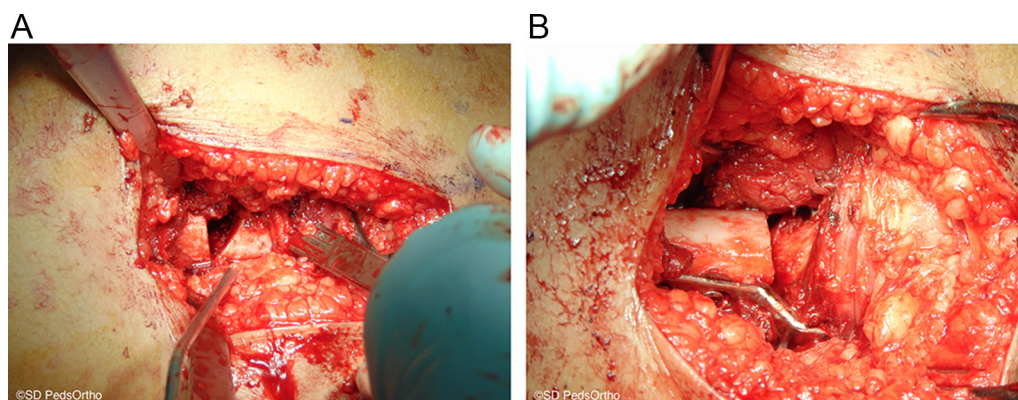


Fig. 2 Imhauser surgical procedure showing: (a) the space left after wedge removal and (b) final reduction with instrumentation.

visualisation of the unique 3D nature of SCFE and improve pre-operative planning, which may result in shorter surgeries, less fluoroscopy exposure and lower complication rate.

Patient-specific 3D models that give the surgeon the opportunity to practice osteotomies before entering the operating room appear to be a valuable method for surgical planning prior to complex skeletal realignment procedures. As an initial pilot (15 patients), this study illustrated that 3D models may decrease surgical time by approximately 45 minutes and cut fluoroscopy time in half while maintaining optimal surgical correction of the 3D SCFE deformity.

Received 21 December 2016; accepted after revision 2 February 2017.

COMPLIANCE WITH ETHICAL STANDARDS

FUNDING STATEMENT

No benefits in any form have been received or will be received from a commercial party related directly or indirectly to the subject of this article.

OA LICENCE TEXT

This article is distributed under the terms of the Creative Commons Attribution-Non Commercial 4.0 International (CC BY-NC 4.0) licence (<https://creativecommons.org/licenses/by-nc/4.0/>) which permits non-commercial use, reproduction and distribution of the work without further permission provided the original work is attributed.

ACKNOWLEDGEMENTS

We thank Daniel P. Arnold and Tailynn S. Chen for their assistance with the 3D printing process.

ETHICAL STATEMENT

All procedures performed in studies involving human participants were in accordance with the ethical standards of the institutional and/or national research committee and with the 1964 Helsinki Declaration and its later amendments or comparable ethical standards. This article does not contain any studies with animals performed by any of the authors.

Informed Consent. A waiver of informed consent was granted from our institutional review board for subjects whose treatment and follow up period was complete prior to the start of this study (the senior group). Informed consent was obtained from all individual participants included in the study whose treatment and follow up period occurred after or overlapped the start of this study.

This study was supported by Rady Children's Orthopedic Research and Education. This material is based upon work supported by the National Science Foundation Graduate Research Fellowship under Grant No. DGE-1144086 (JPC) and by NHLBI of the National Institutes of Health under 5T35HL007491 (LC) and P01 AG007996 (RLS). The content is solely the responsibility of the authors and does not necessarily represent the official views of the National Institutes of Health.

ICMJE CONFLICT OF INTEREST STATEMENT

DRW reports the following disclosures: *Journal of Pediatric Orthopedics* Editorial or governing board. Orthopediatrics: Consultancy. Rhino Orthopedic Designs: Stock or stock Options.

RLS reports the following disclosures: *Cartilage* Editorial or governing board. *Osteoarthritis and Cartilage*: Editorial or governing board
GlaxoSmithKline: Stock or stock Options. Johnson & Johnson: Stock or stock Options. Medtronic: Stock or stock Options. *Orthopaedic Research Society*: Board or committee member

VVU reports the following disclosures: Orthopediatrics: Consultancy; Payment for development of educational presentation including service on speakers' bureaus

REFERENCES

1. **Lehmann CL, Arons RR, Loder RT, Vitale MG.** The epidemiology of slipped capital femoral epiphysis: an update. *J Pediatr Orthop* 2006;26:286-290.
2. **Crawford AH.** Slipped capital femoral epiphysis. *J Bone Joint Surg [Am]* 1988; 70-A:1422-1427.
3. **Schai PA, Exner GU.** Corrective Imhäuser intertrochanteric osteotomy. *Oper Orthop Traumatol* 2007;19:368-388. [In German]
4. **Parsch K, Zehender H, Bühl T, Weller S.** Intertrochanteric corrective osteotomy for moderate and severe chronic slipped capital femoral epiphysis. *J Pediatr Orthop B* 1999;8:223-230.
5. **Witbreuk MMEH, Bolkenbaas M, Mullender MG, Sierevelt IN, Besselaar PP.** The results of downgrading moderate and severe slipped capital femoral epiphysis by an early Imhäuser femur osteotomy. *J Child Orthop* 2009;3:405-410.
6. **Maussen JP, Rozing PM, Obermann WR.** Intertrochanteric corrective osteotomy in slipped capital femoral epiphysis. A long-term follow-up study of 26 patients. *Clin Orthop Relat Res* 1990;259:100-110.
7. **Kartenbender K, Cordier W, Kattagen BD.** Long-term follow-up study after corrective Imhäuser osteotomy for severe slipped capital femoral epiphysis. *J Pediatr Orthop* 2000;20:749-756.
8. **Wenger DR, Bomar JD.** Acute, unstable, slipped capital femoral epiphysis: is there a role for in situ fixation? *J Pediatr Orthop* 2014;34:S11-S17.
9. **Southwick WO.** Osteotomy through the lesser trochanter for slipped capital femoral epiphysis. *J Bone Joint Surg [Am]* 1967;49-A:807-835.
10. **Ziebarth K, Zilkens C, Spencer S, et al.** Capital realignment for moderate and severe SCFE using a modified Dunn procedure. *Clin Orthop Relat Res* 2009;467:704-716.
11. **Souder CD, Bomar JD, Wenger DR.** The role of capital realignment versus in situ stabilization for the treatment of slipped capital femoral epiphysis. *J Pediatr Orthop* 2014;34:791-798.
12. **Herring JA.** Slipped capital femoral epiphysis. In: *Tachdjian's pediatric orthopedics from the Texas Scottish Rite Hospital for Children*. Fifth ed. Philadelphia, PA: Elsevier Health Sciences, 2013:630-665.
13. **Guarino J, Tennyson S, McCain G, et al.** Rapid prototyping technology for surgeries of the pediatric spine and pelvis: benefits analysis. *J Pediatr Orthop* 2007;27:955-960.
14. **Blakeney WG, Day R, Cusick L, Smith RL.** Custom osteotomy guides for resection of a pelvic chondrosarcoma. *Acta Orthop* 2014;85:438-441.
15. **Ma B, Kunz M, Gammon B, Ellis RE, Pichora DR.** A laboratory comparison of computer navigation and individualized guides for distal radius osteotomy. *Int J Comput Assist Radiol Surg* 2014;9:713-724.

16. **Nadler SB, Hidalgo JH, Bloch T.** Prediction of blood volume in normal human adults. *Surgery* 1962;51:224-232.
17. **Gross JB.** Estimating allowable blood loss: corrected for dilution. *Anesthesiology* 1983;58:277-280.
18. **Jarrett DY, Matheney T, Kleinman PK.** Imaging SCFE: diagnosis, treatment and complications. *Pediatr Radiol* 2013;43:S71-S82.
19. **Isaac B, Vettivel S, Prasad R, Jeyaseelan L, Chandi G.** Prediction of the femoral neck-shaft angle from the length of the femoral neck. *Clin Anat* 1997;10:318-323.
20. **Bartoníček J, Skála-Rosenbaum J, Dousa P.** Valgus intertrochanteric osteotomy for malunion and nonunion of trochanteric fractures. *J Orthop Trauma* 2003;17:606-612.
21. **Paley D.** Normal Lower Limb Alignment and Joint Orientation. In: *Principles of deformity correction*. New York: Springer, 2002:1-18.
22. **Klinge K, Samora W.** Treatment of Acute, Unstable versus Chronic, Stable Slipped Capital Femoral Epiphysis using the Modified Dunn Procedure. *Pediatr. Orthop. Soc. North Am*; 2016:161.